J|A|C|S
ARTICLES
Published on Web 12/30/2003

Kinetics of End-to-End Collision in Short Single-Stranded Nucleic Acids

Xiaojuan Wang[†] and Werner M. Nau*[,†,‡]

Contribution from the Departement Chemie, Universität Basel, Klingelbergstrasse 80, CH-4056 Basel, Switzerland, and the School of Engineering and Science, International University Bremen, Campus Ring 1, D-28759 Bremen, Germany

Received September 1, 2003; E-mail: w.nau@iu-bremen.de.

Abstract: A novel fluorescence-based method, which entails contact quenching of the long-lived fluorescent state of 2,3-diazabicyclo[2.2.2]-oct-2-ene (DBO), was employed to measure the kinetics of end-to-end collision in short single-stranded oligodeoxyribonucleotides of the type 5′-DBO−$(X)_n$-dG with X = dA, dC, dT, or dU and $n = 2$ or 4. The fluorophore was covalently attached to the 5′ end and dG was introduced as an efficient intrinsic quencher at the 3′ terminus. The end-to-end collision rates, which can be directly related to the efficiency of intramolecular fluorescence quenching, ranged from 0.1 to 9.0 × 10^6 s^{-1}. They were strongly dependent on the strand length, the base sequence, as well as the temperature. Oligonucleotides containing dA in the backbone displayed much slower collision rates and significantly higher positive activation energies than strands composed of pyrimidine bases, suggesting a higher intrinsic rigidity of oligoadenylate. Comparison of the measured collision rates in short single-stranded oligodeoxyribonucleotides with the previously reported kinetics of hairpin formation indicates that the intramolecular collision is significantly faster than the nucleation step of hairpin closing. This is consistent with the configurational diffusion model suggested by Ansari et al. (Ansari, A.; Kuznetsov, S. V.; Shen, Y. *Proc. Natl. Acad. Sci. USA* **2001**, *98*, 7771−7776), in which the formation of misfolded loops is thought to slow hairpin formation.

Introduction

Recent work on nucleic acid dynamics has focused on the formation of single-stranded DNA (ssDNA) hairpins,[1−8] which are believed to play a key role in many biological functions, including gene expression and regulation,[9−11] DNA transcription,[12,13] as well as DNA transposition.[14] Hairpin formation includes not only the collision of the two arms but also the fast zipping of the stem part. To describe the hairpin-to-coil transition, a two-state model of an all-or-none transition between open and closed states was introduced by Libchaber and coworkers.[1,2] However, the kinetics of hairpin formation displayed a non-Arrhenius temperature dependence in some cases which points to a more complex mechanism.[5,6] Ansari and coworkers[6,7] suggested a configurational diffusion model, in which the ssDNA can be transiently trapped in misfolded states prior to the nucleation step. The test of this model requires experimental end-to-end collision rates in ssDNA, which we are now providing for the first time. To allow a direct comparison, we have studied ssDNA fragments which correspond in their size to the loop segments of the previously studied entire hairpins.

We employed a novel method which uses 2,3-diazabicyclo-[2.2.2]-oct-2-ene (DBO) as a fluorescent probe. The extremely long fluorescence lifetime of DBO (325 ns in aerated water and 420 ns in deaerated water) and its quenching mechanism, which requires a close probe-quencher contact, offer the possibility to monitor intramolecular collisions in the submicrosecond scale which has proven difficult to realize by alternative techniques. A phosphoramidite DBO derivative (**2**) was synthesized and directly applied in automated solid-phase synthesis to obtain 5′-DBO-labeled oligonucleotides (see below). The end-to-end collision rates were measured through the intramolecular fluorescence quenching of DBO by a guanine base as quencher

[†] Departement Chemie, Universität Basel, Klingelbergstrasse 80, CH-4056 Basel, Switzerland.

[‡] School of Engineering and Science, International University Bremen, Campus Ring 1, D-28759 Bremen, Germany.

(1) Bonnet, G.; Krichevsky, O.; Libchaber, A. *Proc. Natl. Acad. Sci. U.S.A.* **1998**, *95*, 8602−8606.
(2) Goddard, N. L.; Bonnet, G.; Krichevsky, O.; Libchaber, A. *Phys. Rev. Lett.* **2000**, *85*, 2400−2403.
(3) Ying, L.; Wallace, M. I.; Klenerman, D. *Chem. Phys. Lett.* **2001**, *334*, 145−150.
(4) Wallace, M. I.; Ying, L.; Balasubramanian, S.; Klenerman, D. *J. Phys. Chem. B* **2000**, *104*, 11 551−11 555.
(5) Wallace, M. I.; Ying, L.; Balasubramanian, S.; Klenerman, D. *Proc. Natl. Acad. Sci. U.S.A.* **2001**, *98*, 5584−5589.
(6) Ansari, A.; Kuznetsov, S. V.; Shen, Y. *Proc. Natl. Acad. Sci. U.S.A.* **2001**, *98*, 7771−7776.
(7) Shen, Y.; Kuznetsov, S. V.; Ansari, A. *J. Phys. Chem. B* **2001**, *105*, 12 202−12 211.
(8) Kuznetsov, S. V.; Shen, Y.; Benight, A. S.; Ansari, A. *Biophys. J.* **2001**, *81*, 2864−2875.
(9) Zazopoulos, E.; Lalli, E.; Stocco, D. M.; Sassone-Corsi, P. *Nature* **1997**, *390*, 311−315.
(10) Goodfellow, P. N.; Camerino, G. *Cell. Mol. Life Sci.* **1999**, *55*, 857−863.
(11) McCaffrey, A. P.; Meuse, L.; Pham, T.-T. T.; Conklin, D. S.; Hannon, G. J.; Kay, M. A. *Nature* **2002**, *418*, 38−39.
(12) Catasti, P.; Chen, X.; Moyzis, R. K.; Bradbury, E. M.; Gupta, G. *J. Mol. Biol.* **1996**, *264*, 534−545.
(13) Soldatenkov, V. A.; Chasovskikh, S.; Potaman, V. N.; Trofimova, I.; Smulson, M. E.; Dritschilo, A. *J. Biol. Chem.* **2002**, *277*, 665−670.
(14) Lee, G. S.; Neiditch, M. B.; Sinden, R. R.; Roth, D. B. *Mol. Cell. Biol.* **2002**, *22*, 2068−2077.

10.1021/ja038263r CCC: $27.50

Scheme 1

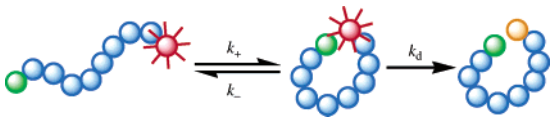

at the 3′ terminus (Scheme 1). The efficient quenching of DBO by guanine ensures that the end-to-end collision in a random-coiled oligonucleotide (k_+ in Scheme 1) is followed by rapid deactivation of the excited state (k_d) before the chain ends dissociate (k_-). In this limiting kinetic scenario, the quenching rate constant (k_q) equals the pertinent rate constant for end-to-end collision (k_+). The k_q values provide therefore a direct measure of the flexibility of the oligonucleotide backbone.

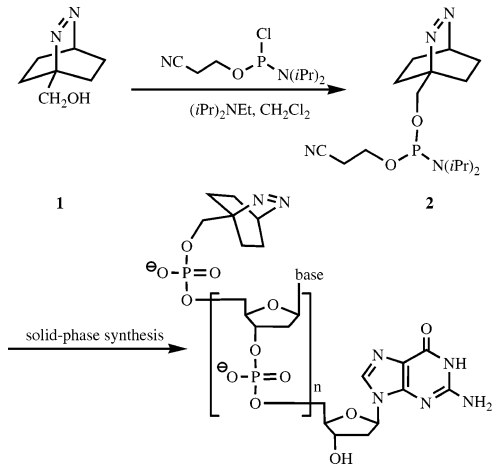

Experimental Section

Materials. Commercial materials were from Fluka or Aldrich. 1-Hydroxymethyl-2,3-diazabicyclo[2.2.2]-oct-2-ene (**1**) was synthesized according to a literature procedure.[15] The primary hydroxyl group was converted to 2-cyanoethyl *N*,*N*-diisopropylphosphoramidite by using the phosphitylating reagent $ClP(OCH_2CH_2CN)N(iPr)_2$. The DBO-labeled oligonucleotides were synthesized by Amplimmun AG (Madulaina, Switzerland) in 1.0 μmol scale in >95% purity; the DBO phosphoramidite (**2**) was coupled to the 5′-terminus of synthetic oligonucleotides during the last stage of the automated solid-phase synthesis. RP-HPLC (5−70% acetonitrile in 0.1 M triethylamine acetate (TEAA)) was used for desalting and removal of failure sequences. The remaining TEAA from the eluant was removed by lyophilization.

Synthesis of DBO-Phosphoramidite (2). A solution of dry 1-hydroxymethyl-2,3-diazabicyclo[2.2.2]-oct-2-ene (**1**, 337 mg, 2.4 mmol) and anhydrous diisopropylethylamine (0.7 mL, 4 mmol) in 16 mL of dichloromethane was stirred under argon. 2-Cyanoethyl *N*,*N*-diisopropylphosphoramidochloridite (0.6 mL, 2.8 mmol) was added dropwise, the mixture was then stirred for 2 h, transferred to a separatory funnel along with 50 mL of ethyl acetate and washed with saturated sodium chloride solution (2 × 40 mL). The organic phase was dried over anhydrous sodium sulfate, filtered, and then rotary-evaporated to yield a yellowish oil. Purification by flash column chromatography (SiO_2, ethyl acetate/dichloromethane/triethylamine 5:5:1) yielded a colorless oil (580 mg, 71%). It was dissolved in ethyl acetate, precipitated from *n*-hexane at −20 °C, filtered off quickly and evaporated to dryness to give **2** as a colorless solid which melts at room temperature (490 mg, 60%). ^{31}P NMR ($CDCl_3$, 400 MHz): δ 145.89 ppm;^{1}H NMR ($CDCl_3$, 400 MHz): δ 1.12−1.20 (m, 2H, CH_2), 1.21 (d, J = 6.8 Hz, 12H, CH_3), 1.31−1.37 (m, 2H, CH_2), 1.57−1.68 (m, 4H, CH_2), 2.65 (dt, J = 6.6, 2.5 Hz, 2H, CH_2CN), 3.60−3.70 (m, 2H, CHN), 3.81−3.94, (m, 2H, CH_2O), 4.12−4.16 (m, 1H, CH_2O), 4.25−4.30 (m, 1H, CH_2O), 5.15 (t, J = 3.5 Hz, 1H, CH) ppm; ^{13}C NMR ($CDCl_3$, 400 MHz): δ 20.8 (CH_2), 21.9 (2C, CH_2), 23.9 (2C, CH_2), 25.0 (4C, CH_3), 43.6 (2C, CHN), 58.9 (CH_2O), 62.3 (CHN), 67.4 (C_q), 69.4 (CH_2O), 118.0 (CN) ppm. FAB−MS (NBA) 340; Calcd 340.4.

Sample Preparation. Concentrations of labeled synthetic oligonucleotides in water were calculated from the absorbance at 260 nm (A_{260}).[16] The fluorescent probe displays a weak absorbance in the near UV (λ_{max} ca. 365 nm, ϵ ca. 50 cm^{-1} M^{-1}) but is transparent at 260 nm,[17] such that no correction for the probe absorption is necessary in the calculation of the oligonucleotide concentration. The strand concentrations in all measurements were adjusted to 60−80 μM, sufficiently low to exclude intermolecular fluorescence quenching.

Fluorescence Measurements. All measurements were performed in aerated water at 25 °C except for the temperature-dependent experiments. Fluorescence decays were recorded on a laser-flash photolysis setup (LP900, Edinburgh Instruments, Edinburgh, Scotland) with 7-mJ, 355-nm pulses of 4 ns width from a Nd:YAG laser (Minilite II, Continuum, Santa Clara, CA), or on a time-correlated single-photon counting (TCSPC) fluorometer (FLS920, Edinburgh Instruments) by using a 1.5-ns pulse-width H_2 flash lamp at 370 nm. Fluorescence was monitored at 440 nm. The resulting data were analyzed by mono-exponential fitting to afford the respective fluorescence lifetimes with typical errors of ±3%.

Results

Selection of Intrinsic Quencher. The quenching methodology in Scheme 1 requires the selection of an efficient fluorescence quencher, which should ideally be an intrinsic component of the respective biopolymer. While in the case of peptides this role can be taken over by the amino acids tryptophan or tyrosine,[18,19] guanine presents the best choice when applying this method to oligonucleotides. In fact, when comparing the bimolecular quenching rate constants of free DBO by different mono-nucleotides[20] the order GMP (dGMP) > dTMP > UMP ≈ CMP (dCMP) ≫ AMP (dAMP) results, with GMP (dGMP) yielding a high rate constant of 5.0×10^8 $M^{-1}s^{-1}$ in aerated water, 40 times faster than the quenching rate of AMP (dAMP), but less than the diffusion-controlled limit.

Diffusion coefficients of probe and quencher when covalently linked to a biopolymer should fall at least 1 order of magnitude below the values for intermolecular diffusion of free molecules.[21−23] This is due to the movement restriction and the internal friction imposed by the chain backbone. As a result, intramolecular reactions between a probe and a quencher may be controlled by intrachain diffusion even if the rate of the corresponding intermolecular reaction falls up to 1 order of magnitude below the diffusion-controlled limit like for the dGMP/DBO pair. Consequently, it is reasonable to assume that the *intramolecular* quenching process between DBO and guanine is collision-controlled,[24] i.e., quenching occurs before

(15) Zhang, X.; Gramlich, G.; Wang, X.; Nau, W. M. *J. Am. Chem. Soc.* **2002**, *124*, 254−263.
(16) Borer, P. N. *Handbook of Biochemistry and Molecular Biology*, 3rd ed.; CRC Press: Cleveland, 1975.
(17) Nau, W. M.; Wang, X. *ChemPhysChem* **2002**, *3*, 393−398.
(18) Hudgins, R. R.; Huang, F.; Gramlich, G.; Nau, W. M. *J. Am. Chem. Soc.* **2002**, *124*, 556−564.
(19) Huang, F.; Nau, W. M. *Angew. Chem., Int. Ed. Engl.* **2003**, *42*, 2269−2272.
(20) Marquez, C.; Pischel, U.; Nau, W. M. *Org. Lett.* **2003**, *5*, 3911−3914.
(21) Lapidus, L. J.; Eaton, W. A.; Hofrichter, J. *Proc. Natl. Acad. Sci. U.S.A.* **2000**, *97*, 7220−7225.
(22) Hagen, S. J.; Hofrichter, J.; Eaton, W. A. *J. Phys. Chem. B* **1997**, *101*, 2352−2365.
(23) Liu, G.; Guillet, J. E.; Al-Takrity, E. T. B.; Jenkins, A. D.; Walton, D. R. M. *Macromolecules* **1990**, *23*, 4164−4167.

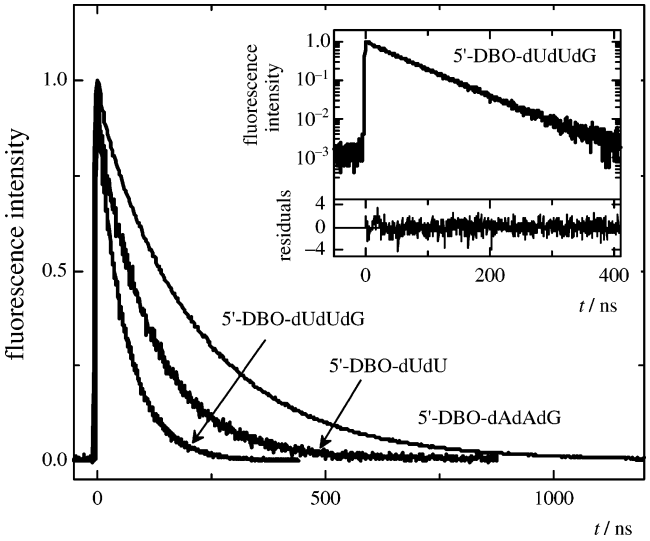

Figure 1. Fluorescence decays of DBO-labeled ssDNA (normalized intensity, recorded by TCSPC). Shown in the inset is a fluorescence decay on a semilogarithmic scale.

the probe/quencher pair dissociates ($k_d \gg k_-$). The deactivation mechanism of DBO by guanine is presumed to be direct or exciplex-mediated quenching by N−H hydrogen abstraction[17,25−27] as evidenced by the significant solvent deuterium isotope effect of 1.4.[20] This quenching by hydrogen atom transfer requires a close probe/quencher contact, another important requirement for applying the methodology in Scheme 1.

Fluorescence Quenching by End-to-End Collisions. Sequences of single-stranded oligonucleotides were designed as 5′-DBO−$(X)_n$-dG, where X = dC, dT, dU, or dA and $n = 2$ or 4. At room temperature, these oligonucleotides do not possess a stable secondary structure (random coil, cf. Scheme 1) although base-stacking interactions are partly maintained between purine bases.[28,29] Solutions of the oligonucleotides displayed monoexponential fluorescence decays (Figure 1), i.e., each oligonucleotide has a specific "fluorescence lifetime", τ_{obs}, similar to the situation for DBO-labeled polypeptides[18,19] and consistent with recent numerical simulations.[30]

The excited DBO decays through three channels: (*i*) quenching upon contact with guanine at the other end through mutual diffusion of the chain ends, (*ii*) quenching upon contact with bases in the backbone (mainly the nearest neighboring nucleotide), and (*iii*) the inherent decay through fluorescence and nonradiative processes. To extract the first component, i.e., the kinetics of end-to-end collision, reference strands with identical sequence but without the 3′ terminal quencher (5′-DBO−$(X)_n$) were measured in all cases; the fluorescence lifetime of these reference strands (τ_0) reflects only the last two kinetic components (*ii*) and (*iii*), since the nature of the backbone is retained. The quenching rate constants related to quenching by guanine (k_q) can then be obtained according to eq 1, which corresponds, subject to the assumption of nearly-quantitative quenching upon contact ($k_d \gg k_-$), to the rate of end-to-end collision (k_+ in eq 2)

$$k_q = \frac{1}{\tau_{obs}} - \frac{1}{\tau_0} \quad (1)$$

$$k_q = \frac{k_+ k_d}{k_d + k_-} \approx k_+, \text{ for } k_d \gg k_- \quad (2)$$

In the actual experiments, there is a significant decrease of the fluorescence lifetime when guanine is attached, i.e., $\tau_{obs} < \tau_0$. In the case of 5′-DBO-$(dU)_2$-dG and 5′-DBO−$(dU)_2$ (Figure 1), for example, the lifetimes are 58 ns (τ_{obs}) and 120 ns (τ_0), respectively, corresponding to $k_q = 9.0 \times 10^6\ s^{-1}$.[31] The lifetime shortening is due to the efficient quenching by dG and the conformational fluctuation of the flexible backbone which allows the chain ends to reach conformations where end-to-end contact is possible (cf. Discussion).

Table 1. Rate Constants and Activation Energies for End-to-End Collision in Single-Stranded Oligonucleotides

oligonucleotide	τ_{obs}/ns	τ_0/ns[a]	$k_+/(10^6\ s^{-1})$[b]	E_a/(kJ/mol)[c]	log$A$[d]
5′-DBO-dAdA-dG	215	243	0.54	43	13.3
5′-DBO-dTdT-dG	60	94	6.0	14	9.2
5′-DBO-dCdC-dG	67	123	6.7	14	9.3
5′-DBO-dUdU-dG	58	120	9.0	12	9.0
5′-DBO-dAdC-dG	106	162	3.2	20	10.0
5′-DBO-dAdAdAdA-dG	247	255	0.12	33	10.9
5′-DBO-dTdTdTdT-dG	72	87	2.4	14	9.0
5′-DBO-dCdCdCdC-dG	96	115	1.8	16	9.0
5′-DBO-dUdUdUdU-dG	83	118	3.6	10	8.3
5′-DBO-dAdCdAdC-dG	131	164	1.5	15	8.7

[a] τ_0 is the lifetime of the reference strand with identical sequence but without the 3′ terminal dG as quencher, 5′-DBO-$(X)_n$. [b] At 25 °C, error in data is 10%. [c] Temperature range 25−40 °C; error in data is ±3 kJ/mol. [d] Temperature range 25−40 °C; error in data is 20%.

Rate Constants and Activation Energies for End-to-End Collision in ssDNA. The intramolecular quenching rate constants for ssDNA containing a backbone of different length composed of different types of nucleotides were determined in a temperature range between 25 and 40 °C (Table 1). It was found that the longer strands ($n = 4$) show slower end-to-end collision rates than the shorter strands ($n = 2$), with a typical factor of 2−4 difference. This length dependence is in line with expectations for end-to-end collision processes in (bio)polymers,[30] and was previously observed for polypeptides.[18] In contrast to the polypeptides, however, we did not observe slower rates for the shortest derivative, i.e., the end-to-end collision rate constant for the shortest homologue in which probe and quencher are directly attached to each other ($n = 0$, 5′-DBO-dG) is the fastest ($\tau_{obs} = 29$ ns, $k_q = 33 \times 10^6\ s^{-1}$). Moreover, the end-to-end collision rates are strongly dependent on the kind of nucleotide in the backbone with the order dU > dT ≈ dC ≫ dA. Again, this is similar to the situation for polypeptides, where

(24) If intramolecular fluorescence quenching of DBO by guanine in oligonulceotides were not fully controlled by intrachain diffusion, the extrapolated end-to-end collision rates could be somewhat larger, which would, in fact, further strengthen our principal conclusion with respect to the mechanism of ssDNA hairpin formation.

(25) Nau, W. M.; Greiner, G.; Rau, H.; Wall, J.; Olivucci, M.; Scaiano, J. C. *J. Phys. Chem. A* **1999**, *103*, 1579−1584.
(26) Pischel, U.; Zhang, X.; Hellrung, B.; Haselbach, E.; Muller, P.-A.; Nau, W. M. *J. Am. Chem. Soc.* **2000**, *122*, 2027−2034.
(27) Pischel, U.; Nau, W. M. *J. Am. Chem. Soc.* **2001**, *123*, 9727−9737.
(28) Mills, J. B.; Vacano, E.; Hagerman, P. J. *J. Mol. Biol.* **1999**, *285*, 245−257.
(29) Saenger, W. *Principles of Nucleic Acid Structure*; Springer-Verlag: New York, 1984.
(30) Wang, X.; Bodunov, E. N.; Nau, W. M. *Opt. Spectrosc.* **2003**, *95*, 560−570.

(31) The question arises whether the lifetime of 5′-DBO-$(dU)_3$ is a more suitable reference for 5′-DBO-$(dU)_2$-dG than 5′-DBO-$(dU)_2$. However, since the lifetimes of 5′-DBO-$(dU)_2$ (120 ns) and 5′-DBO−$(dU)_4$ (118 ns) are virtually the same (Table 1), the length of the reference oligonucleotide appears to be no critical parameter.

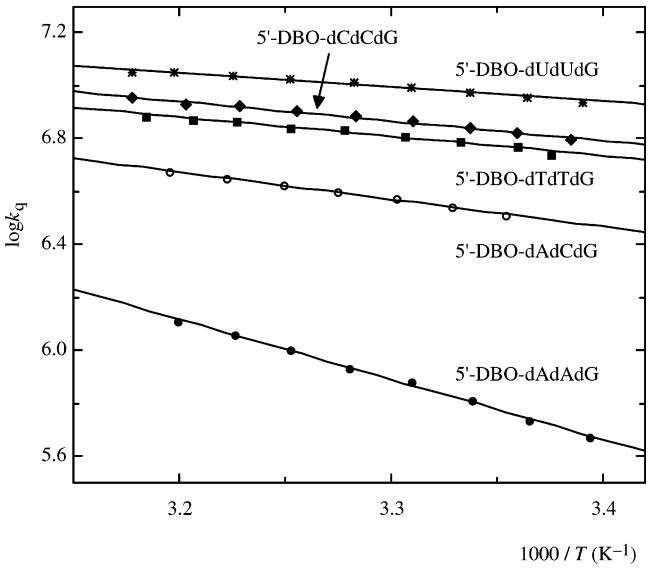

Figure 2. Arrhenius plots of the quenching rate constants in DBO-labeled ssDNA.

the type of amino acid in the backbone is also a crucial parameter in determining the flexibility.

The rate data in Table 1 reveal that about 10^6 collisions occur per second between the chain ends of short ssDNA fragments. Electron transport through DNA, which has attracted significant attention due to its importance for DNA damage and repair, has been reported to occur in ssDNA at a rate of ca. 10^6 s^{-1} with two intervening dT between electron donor and acceptor.[32] This is quite similar to the rate constants for end-to-end collision determined herein, which supports the suggestion that electron transport in ssDNA may proceed through intrachain contact.[32,33]

The intramolecular collision rate constants measured for pyrimidine-derived oligonucleotides ($1.8-9.0 \times 10^6$ s^{-1}) fall up to 1 order of magnitude below those for flexible polypeptides with the same number of monomer units (e.g., 3.3 and 2.5×10^7 s^{-1} for Trp-(Ser)$_4$-DBO and Trp-(Ala)$_4$-DBO in D_2O). The end-to-end collision rate for tetraadenylate (1.2×10^5 s^{-1}) is also 1 order of magnitude slower than those for relatively rigid peptides (e.g., 3.7 and 2.6×10^6 s^{-1} for Trp-(Val)$_4$-DBO and Trp-(Ile)$_4$-DBO in D_2O).[19,34] Oligonucleotides are apparently more rigid than polypeptides. This result may not be further surprising but because the experimental data for intramolecular contact formation in oligonucleotides were previously unavailable, the end-to-end collision rates of ssDNA have been presumed to be similar to those of flexible polypeptides.[7] The present experimental data demonstrate that these biopolymers differ substantially with respect to their flexibility as assessed through the relative mobility of the chain ends.

Arrhenius plots (Figure 2) afforded the activation energy for intramolecular fluorescence quenching of DBO by guanine (E_a, Table 1), which should reflect the energy required for those conformational changes which bring the two chain ends in a short oligonucleotide into contact. All measured activation energies were positive. This is a nontrivial result, because apparent negative activation energies have been reported for ssDNA hairpin formation.[5,6] The activation energies for dU, dT, and dC strands were all close to 16 kJ/mol, the activation energy for solvent viscous flow in H_2O.[35] This suggests immediately that end-to-end collision is limited by solvent friction and only modulated through a probability factor which differentiates the types of nucleotides. The latter could derive from variations in the conformational freedom for bond rotations as imposed by the different steric demand of the bases.

In contrast, end-to-end collision in oligoadenylates displayed significantly higher activation energies, 43 kJ/mol for 5′-DBO-(dA)$_2$-dG and 33 kJ/mol for 5′-DBO−(dA)$_4$-dG, which point to a higher intrinsic 'rigidity' of oligoadenylates. Clearly, end-to-end collision in oligoadenylate is limited by internal friction (not by solvent friction as for the pyrimidine strands), which provides also strong support for the assumption that the intramolecular quenching of DBO by guanine in oligonucleotides is determined by intrachain diffusion (k_+ in Scheme 1), not by an intrinsic activation barrier for excited-state deactivation (k_d).

Because it is known that adjacent adenines can undergo base-stacking interactions,[28,29] two additional ssDNA were investigated, in which the adenine bases in the strands were replaced by cytosine in an alternating manner (see data for 5′-DBO-dAdC-dG and 5′-DBO-dAdCdAdC-dG in Table 1). End-to-end collision in these strands became significantly faster and the rate constants were on the same order of magnitude as those for oligopyrimidines. In addition, the activation energies of end-to-end collision in these oligonucleotides were much smaller than those of oligoadenylates and close to the activation energy of solvent viscous flow.

Discussion

Although experimental data for end-to-end collision rates have recently been reported for polypeptides,[18,19,21,36] the characteristic time scale for intrachain collision in single-stranded nucleic acids has remained elusive. We have now transferred to oligonucleotides the methodology of using intramolecular fluorescence quenching of DBO to obtain the kinetics of intrachain diffusion. The principle of measuring end-to-end collision rates by fluorescence quenching is shown in Scheme 1. This method requires not only a long-lived fluorescent probe to allow quenching through the relatively slow (ns−μs time scale) intrachain diffusion to compete with spontaneous deactivation but requires also a contact quenching mechanism to relate the kinetics of quenching directly to the kinetics of end-to-end collision. Both requirements are fulfilled for the DBO chromophore.[17] In the case of polypeptides, tryptophan was selected as quencher.[18,19] In single-stranded oligonucleotides, guanine can take over this role. Both are the most efficient intrinsic fluorescence quenchers of DBO among natural amino acids and nucleobases, respectively. In view of the comprehensive mechanistic information established in the course of the polypeptide

(32) Meggers, E.; Dussy, A.; Schafer, T.; Giese, B. *Chem. Eur. J.* **2000**, *6*, 485−492.
(33) Kan, Y.; Schuster, G. B. *J. Am. Chem. Soc.* **1999**, *121*, 10 857−10 864.
(34) The fact that Trp is a better intermolecular quencher of DBO fluorescence ($k_q = 21 \times 10^8$ M^{-1}s^{-1}) than guanine ($k_q = 5.0 \times 10^8$ M^{-1}s^{-1}) cannot be responsible for the observed large difference in intramolecular quenching rate constants between peptides and oligonucleotides. When Tyr is used as quencher in peptides, which is similarly efficient ($k_q = 5.6 \times 10^8$ M^{-1}s^{-1}) as guanine, the difference remains, with the rates in peptides being reduced by a factor of 2−3.
(35) The activation energy of solvent viscous flow in H_2O in the relevant temperature range (298−313 K) was obtained by plotting lnη versus 1/T with the viscosities taken from Cho, C. H.; Urquidi, J.; Singh, S.; Robinson, G. W. *J. Phys. Chem. B* **1999**, *103*, 1991−1994.
(36) Bieri, O.; Wirz, J.; Hellrung, B.; Schutkowski, M.; Drewello, M.; Kiefhaber, T. *Proc. Natl. Acad. Sci. U.S.A.* **1999**, *96*, 9597−9601.

studies[37] and in view of additional control experiments performed for ssDNA (cf. Supporting Information), we interpret the intramolecular quenching rate constants (k_q) of the DBO/guanine probe/quencher pair in oligonucleotides in terms of end-to-end collision rate constants (k_+ in Scheme 1) according to eq 2.

The quenching rate data in Table 1 provide the first direct experimental measure of the collision rates between the chain ends in single-stranded oligonucleotides. The slow collision rates for the oligoadenylates stand out and the related strands show also significantly higher activation energies than the oligopyrimidine strands. Because the DNA strands presently employed cannot form intramolecular hydrogen bonds or stable secondary structures, the energy barrier for the quenching process is a measure of the energy required for the conformational changes of the oligonucleotide backbone which bring the probe and quencher into contact. This energy barrier is a composite of the apparent activation energy for solvent viscous flow and the energy barrier of internal friction, i.e., the bond rotations required for end-to-end collision.

It is appropriate to argue, akin to the situation for peptides,[19] that strands whose ends collide with the slowest rates are the most rigid ones. This means that the kinetics of end-to-end collision in ssDNA provides also a direct measure of their intrinsic flexibility. The 10 times slower end-to-end collision rates and the substantial activation energies signal therefore a higher 'rigidity' of oligoadenylates, which is qualitatively consistent with the trend observed by Hagerman and co-workers through persistence length measurements.[28] This increased rigidity is presumably due to two reasons. On one hand, purine bases are larger than pyrimidines, which decreases the intrachain diffusion coefficient and imposes higher steric restrictions toward bond rotation. On the other hand, adjacent purine bases undergo sizable base-stacking interactions,[28,29] which impose a barrier toward free bond rotation.

To evaluate the relative importance of these two factors (steric hindrance versus base-stacking interaction) control experiments were performed with 5′-DBO-dAdC-dG and 5′-DBO-dAdCdAdC-dG strands, in which the purine base stacking is destroyed by the alternating cytosine bases.[2,38] These strands show much faster rate constants and also smaller activation energies for end-to-end collision than the homogeneous dA strands (Table 1), which suggests that the major contributor to the rigidity of the oligoadenylates strands is due to base stacking. However, the rate constants and activation energies do not quite reach the values for the pyrimidine strands, which indicates that the larger size of adenine and the related steric hindrance involved during conformational changes has an effect as well. The control experiments with the mixed purine/pyrimidine strands immediately demonstrate that the flexibility of DNA fragments cannot be predicted in an incremental fashion from the flexibility of strands containing only identical bases, but that synergetic effects, in particular base-stacking interactions between neighboring purine bases, operate.

The measured activation energy for end-to-end collision in 5′-DBO-$(dA)_2$-dG suggests that the destruction of base-stacking interaction in an AAG unit may require as much as 30−40 kJ/mol, which compares well with the stabilization energy of a single AA base stack obtained by molecular modeling (34 kJ/mol).[38] Interestingly, the activation energy for the longer adenine strand, 5′-DBO-$(dA)_4$-dG, is *smaller* than that of the shorter one. Presumably, the conformation for end-to-end contact formation in 5′-DBO-$(dA)_4$-dG has a larger circle radius, which renders steric hindrance effects less important and which may even allow the base-stacking interaction to be partially retained during the collision process. This trend is consistent with the analysis of Ansari and co-workers which implies that the energetic cost of bending a molecular chain to a loop should decrease with increasing length.[7]

The flexibility of DNA is deemed important in additional key events, including electron transfer[32,33,39] as well as nucleic acid−protein selective binding.[40−42] In fact, the higher intrinsic rigidity of single-stranded oligoadenylates observed in the present study may provide a possible explanation for the reduced binding of the SSB protein with poly(dA), compare binding enthalpies of −14 kcal/mol for poly(dA), −75 kcal/mol for poly(dT), and −85 kcal/mol for poly(dC).[43] The binding to the protein requires a substantial conformational change of the ssDNA, the energetic cost of which is highest in poly(dA) due to the required unstacking, cf. activation energies in Table 1.

Oligopyrimidines do not show substantial base-stacking interactions at room temperature.[28,44] Our observations that the end-to-end collision rates of strands composed of dT, dU, and dC differed weakly and the activation energies were all close to 16 kJ/mol, the activation energy of the solvent viscous flow in water,[35] indicated that the friction with solvent molecules during conformational changes is the main contributor to the energy barrier. This applies both for the shorter ($n = 2$) as well as the longer ($n = 4$) oligonucleotides studied. The differences between the absolute rate constants for dT and dU strands are small, but nevertheless consistent with their molecular structure. The faster quenching of dU relative to dT strands can be related to the lack of the extra methyl group which will exhibit increased steric hindrance effects in the course of the required bond rotations in dT strands. A general relationship between the size of the residue in the chain segments and the rate of end-to-end collision has already been recognized in polypeptides, where larger residues also tend to slow this process.[19]

The absolute rate constants for end-to-end collision in ssDNA are essential for the understanding of the mechanism of ssDNA hairpin formation.[1−8] In particular, these elementary rate data can provide information on whether it is the kinetics of end-to-end contact formation that is rate-determining for hairpin formation. An ssDNA hairpin is composed of a single-stranded loop part and a double-stranded stem part with several base pairs. Ansari and co-workers have suggested that the rate-determining step in hairpin formation is the formation of a loop with a 'correct' base pair.[6,7] They argued that only a 'correct' nucleating loop can result in rapid zipping of the hairpin, but that intrachain collisions in ssDNA can also form misfolded loops which do not lead to subsequent zipping of the stem part and thereby

(37) Nau, W. M.; Huang, F.; Wang, X.; Bakirci, H.; Gramlich, G.; Marquez, C. *Chimia* **2003**, *57*, 161−167.
(38) Aalberts, D. P.; Parman, J. M.; Goddard, N. L. *Biophys. J.* **2003**, *84*, 3212−3217.
(39) O'Neill, M. A.; Barton, J. K. *J. Am. Chem. Soc.* **2002**, *124*, 13 053−13 066.
(40) Hogan, M. E.; Roberson, M. W.; Austin, R. H. *Proc. Natl. Acad. Sci. U.S.A.* **1989**, *86*, 9273−9277.
(41) Hogan, M. E.; Austin, R. H. *Nature* **1987**, *329*, 263−266.
(42) Suck, D. *Biopolymers* **1997**, *44*, 405−421.
(43) Kozlov, A. G.; Lohman, T. M. *Biochemistry* **1999**, *38*, 7388−7397.
(44) Camerman, N.; Fawcett, J. K.; Camerman, A. *J. Mol. Biol.* **1976**, *107*, 601−621.

reduce the hairpin formation rate. Their results showed that the closing rate for a DNA hairpin with 4 dT in the loop is ca. 0.8×10^5 s^{-1} (25 °C).[6] Our experiments afforded an end-to-end collision rate of 2.4×10^6 s^{-1} for 5′-DBO-$(dT)_4$-dG, which is much faster and suggests that the time for hairpin formation is 'longer' than expected from the time of forming a loop. This result is consistent with the idea that not all end-to-end or other intrachain contacts induce hairpin formation, i.e., there are mismatches and inefficient contacts, which require the ssDNA to explore several local minima conformations until the 'correct' nucleating loop is reached. The absolute rate constants for end-to-end collision in oligonucleotides provide therefore strong support for the configurational diffusion model by Ansari and co-workers.

Moreover, previous work on the formation of DNA hairpins[5,6] have afforded *negative* activation energies for the folding rates, which are in contrast to the positive activation energy of end-to-end collision rates reported herein. This contrast provides further support that hairpin formation, unlike end-to-end collision of random-coiled oligonucleotides, involves a transition state with lower enthalpy than the initial state.[6,45] In terms of the model by Ansari and co-workers, the initial state corresponds to the random-coiled ssDNA and the apparent transition state is the loop in which a single correct base pair is formed; the hydrogen bonds in this base pair stabilize the transition state, which provides the underlying reason for the measured negative activation energy. The oligonucleotides in our systems cannot form stable base pairs during end-to-end collision, such that a positive activation energy results, which is characteristic for the temperature dependence of the solvent viscosity and the energy required for conformational changes, including the unstacking of purine bases.

Finally, it is noteworthy that the absolute rates for end-to-end collision in oligonucleotides as well as peptides are also manifested in the kinetics of secondary structure formation. For example, the presently reported rates for oligonucleotides are 1 order of magnitude slower than those for polypeptides with the same number of residues,[18,19] suggesting a relatively higher 'rigidity' of oligonucleotides. This is in fact reflected also in the rates for hairpin formation in oligonucleotides as well as in peptides, with the latter (as β-hairpins) being formed 1 order of magnitude faster.[1,5,46]

Conclusions

We have shown that the end-to-end collision rates of short ssDNA can be experimentally measured by employing a fluorescence-based method, in which the end-attached chromophore DBO is efficiently quenched upon contact with dG at the other end. These elementary kinetic data are essential to predict the time scale and determine the mechanism of secondary structure formation, e.g., for hairpins, to evaluate the rigidity of different base sequences, and they provide benchmark values for the development of computational methods for ssDNA dynamics. The present experiments in dependence on temperature and base sequence show that oligoadenylate is much more rigid than the oligonucleotides composed of pyrimidines, which is mainly due to the base-stacking interactions in oligoadenylate. Compared to the kinetics of DNA hairpin formation, which has been previously studied, the end-to-end collision rate of the oligonucleotide corresponding to the hairpin loop part is 1 order of magnitude faster. This contrast indicates that the effective intrachain diffusion is strongly slowed during hairpin formation, which supports the configurational diffusion model, where misfolded loops are presumed to slow hairpin formation.

Acknowledgment. This study was performed within the Swiss National Research Program "Supramolecular Functional Materials" (NRP 47, Grant No. 4047-057552) and supported by the Schweizerischer Nationalfonds (Grant No. 620-58000).

Supporting Information Available: Control experiments to establish methodology. This material is available free of charge via the Internet at http://pubs.acs.org.

JA038263R

(45) Eaton, W. A.; Munoz, V.; Hagen, S. J.; Jas, G. S.; Lapidus, L. J.; Henry, E. R.; Hofrichter, J. *Annu. Rev. Biophys. Biomol. Struct.* **2000**, *29*, 327−359.

(46) Munoz, V.; Henry, E. R.; Hofrichter, J.; Eaton, W. A. *Proc. Natl. Acad. Sci. U.S.A.* **1998**, *95*, 5872−5879.